Radionuclide Therapy of HER2-Positive Microxenografts Using a ^{177}Lu-Labeled HER2-Specific Affibody Molecule

Vladimir Tolmachev,[1,2,3] Anna Orlova,[1,2] Rikard Pehrson,[1,2] Joakim Galli,[1] Barbro Baastrup,[1] Karl Andersson,[2] Mattias Sandström,[3] Daniel Rosik,[1] Jörgen Carlsson,[2] Hans Lundqvist,[2] Anders Wennborg,[1] and Fredrik Y. Nilsson[1,2]

[1]Affibody AB, Bromma, Sweden; [2]Division of Biomedical Radiation Sciences, Uppsala University; and [3]Department of Hospital Physics, Uppsala University Hospital, Uppsala, Sweden

Abstract

A radiolabeled anti-HER2 Affibody molecule ($Z_{HER2:342}$) targets HER2-expressing xenografts with high selectivity and gives good imaging contrast. However, the small size (~7 kDa) results in rapid glomerular filtration and high renal accumulation of radiometals, thus excluding targeted therapy. Here, we report that reversible binding to albumin efficiently reduces the renal excretion and uptake, enabling radiometal-based nuclide therapy. The dimeric Affibody molecule $(Z_{HER2:342})_2$ was fused with an albumin-binding domain (ABD) conjugated with the isothiocyanate derivative of CHX-A″-DTPA and labeled with the low-energy β-emitter ^{177}Lu. The obtained conjugate [CHX-A″-DTPA-ABD-$(Z_{HER2:342})_2$] had a dissociation constant of 18 pmol/L to HER2 and 8.2 and 31 nmol/L for human and murine albumin, respectively. The radiolabeled conjugate displayed specific binding to HER2-expressing cells and good cellular retention *in vitro*. *In vivo*, fusion with ABD enabled a 25-fold reduction of renal uptake in comparison with the nonfused dimer molecule $(Z_{HER2:342})_2$. Furthermore, the biodistribution showed high and specific uptake of the conjugate in HER2-expressing tumors. Treatment of SKOV-3 microxenografts (high HER2 expression) with 17 or 22 MBq ^{177}Lu-CHX-A″-DTPA-ABD-$(Z_{HER2:342})_2$ completely prevented formation of tumors, in contrast to mice given PBS or 22 MBq of a radiolabeled non–HER2-binding Affibody molecule. In LS174T xenografts (low HER2 expression), this treatment resulted in a small but significant increase of the survival time. Thus, fusion with ABD improved the *in vivo* biodistribution, and the results highlight ^{177}Lu-CHX-A″-DTPA-ABD-$(Z_{HER2:342})_2$ as a candidate for treatment of disseminated tumors with a high level of HER2 expression. [Cancer Res 2007;67(6):2773–82]

Introduction

Despite impressive progress in the therapy of localized cancer, the possibility to control disseminated disease is limited. Chemotherapy can be efficient, but the lack of specificity often causes an indiscriminate toxicity. A possible way to reduce the toxicity is to selectively accumulate cytotoxic substances in malignant tumors by targeting molecular structures, which are aberrantly expressed by the cancer cells. The use of radionuclides as a cytotoxic payload can be of advantage because the phenomenon of multidrug resistance is unknown for radionuclides and because of the so-called cross-fire effect (i.e., irradiation of cancer cell by nuclides delivered to their malignant neighbors; ref. 1). The radionuclide-labeled anti-lymphoma antibodies Zevalin (^{90}Y) and Bexxar (^{131}I) showed clear improvement in response rates in comparison with nonradiolabeled counterparts (2, 3), but targeted radionuclide therapy of solid tumors has thus far not achieved a decisive breakthrough. This could partially be explained by the fact that solid tumors are generally more radioresistant than lymphomas. However, the major problem is that existing methods cannot provide the required level of radioactivity accumulation in tumors without delivering unacceptably high doses to critical organs, especially to bone marrow (4). The slow blood clearance and the slow extravasation and tumor penetration are limiting factors of intact immunoglobulins, which have mainly been used as targeting agents in radionuclide therapy. To improve tumor-to-nontumor dose ratios by improving extravasation and interstitial diffusion, smaller antibody fragments (5, 6) and peptide ligands to receptors that are overexpressed in tumors (7) have been considered as targeting agents for radionuclide therapy.

We have recently reported on tumor targeting of a HER2-specific molecule derived from a new class of affinity proteins called Affibody molecules (8, 9). Affibody molecules are small, very stable, 58-amino-acid residue protein domains derived from one of the IgG-binding domains of staphylococcal protein A. The three-helix bundle structure has been used as scaffold for construction of combinatorial libraries, from which Affibody molecule variants that target desired molecules can be selected (10, 11).

Overexpression of the oncogene HER2 (human epidermal growth factor receptor 2, *c-erbB2, neu*) is considered a part of the malignant phenotype and has been detected in a number of malignant tumors, such as carcinomas of breast, ovary, and urinary bladder (12–14). A monoclonal antibody directed against HER2 (trastuzumab) is a registered therapeutic for breast cancer (15), and a number of small-molecule kinase inhibitors (16) and vaccine strategies (17) are in clinical development. HER2 is also considered as a promising target for radionuclide therapy of, for example, breast cancer (18), and both HER2-recognizing antibodies and their fragments have been evaluated in this context (19–23).

We considered that the small size (~7 kDa) and high affinity (K_D = 22 pmol/L) of the anti-HER2 Affibody molecule would enable quick extravasation and tumor penetration as well as provide strong binding to the tumor-associated antigen. Indeed,

Note: The phrase "Affibody molecule" is used in this publication instead of "Affibody® molecule." Affibody® is a trademark owned by Affibody AB. Affibody® is a trademark registered in Sweden, the European Union, and the United States and under trademark application in Japan.

Requests for reprints: Fredrik Y. Nilsson, Affibody AB, Box 20137, 16102 Bromma, Sweden. Phone: 468-5988-3851; E-mail: fredrik.nilsson@affibody.com.

doi:10.1158/0008-5472.CAN-06-1630

high tumor-to-nontumor ratios were obtained for the anti-HER2 Affibody molecule labeled with isotopes of iodine (9, 24), bromine (25), technetium (26), and indium (27). Although all labeling technologies enabled high-contrast gamma camera imaging of HER-2 expression in tumor xenografts, radiometal accumulation in kidneys was high. This may be acceptable for imaging purposes but could be associated with toxicity problems in radiotherapeutic applications.

We hypothesized that it should be possible to reduce the kidney accumulation by associating the radiolabeled Affibody molecule to serum albumin. Albumin (molecular mass, 67 kDa) is present at 50 mg/mL (600 μmol/L) in human and murine plasma (28) and has a long half-life. The pharmacokinetics of small proteins and peptides have been modified by making fusions to albumin (29–31). A technically simpler and possibly more attractive approach is based on reversible noncovalent binding to the patient's own serum albumin (32, 33). We chose to work with an albumin-binding domain (ABD), a monovalent variant of an albumin-binding motif of streptococcal protein G (32). Fusing the Affibody molecule to ABD permits binding of the fusion protein to the patient's own serum albumin following administration, thereby prolonging plasma half-life and reducing uptake in kidneys. As there are several ABD variants with different affinities for albumin available (34), one could foresee modifications of pharmacokinetics by manipulating the affinity of ABD to albumin. Serum albumin extravasates, and the major portion is interstitially located. Furthermore, the combined molecular weight of albumin and the Affibody construct used in this study [ABD-$(Z_{HER2:342})_2$, ~87 kDa] is less than the molecular weigh of IgG or its $(Fab')_2$ fragment. Together with an expected free, non–albumin-bound fraction of ABD-$(Z_{HER2:342})_2$, with size 20 kDa, this could provide for a more efficient extravasation and diffusion in the tumor interstitium.

The goal of this study was to evaluate if fusing the anti-HER2 Affibody molecule $Z_{HER2:342}$ to the ABD could improve the pharmacokinetics and enable radionuclide therapy of very small HER2-expressing tumors. As the most appropriate application for targeted radionuclide therapy of solid tumors is minimal residual disease (4, 35), radionuclides with low β energy should be most suitable as labels. Among commercially available nuclides, ^{177}Lu ($T_{1/2}$ = 7.7 days, <Eβ> = 133 keV) and ^{131}I ($T_{1/2}$ = 8.02 days, <Eβ> = 182 keV) can be considered as the most suitable for this application, both in terms of emitted radiation and half-life.

Materials and Methods

Production of $(Z_{HER2:342})_2$ and ABD-$(Z_{HER2:342})_2$. A DNA fragment encoding $Z_{HER2:342}$ was PCR-amplified and subcloned in two pET (Novagen, Madison, WI) derived expression vectors (pAY492 and pAY540). The molecule was subcloned in dimeric form by using the restriction enzyme *Acc*I. The pAY540 vector contains the gene for ABD located upstream of the *Acc*I cloning site. The resulting vector pAY773 encodes the bivalent Affibody molecule $(Z_{HER2:342})_2$, and pAY770 encodes $(Z_{HER2:342})_2$ in fusion with a NH_2-terminal ABD.

The resulting pAY770 [ABD-$(Z_{HER2:342})_2$] and pAY773 [$(Z_{HER2:342})_2$] were transformed to chemocompetent *Escherichia coli* strain BL21(DE3) (Novagen). ABD-$(Z_{HER2:342})_2$ was expressed in shaker flasks; the cell pellet was disrupted through sonication; and the protein was affinity purified using in-house coupled human serum albumin on CNBr-activated Sepharose 4FF (Amersham Biosciences AB, Uppsala, Sweden) and reverse-phase column, RESOURCE RPC 3 mL (Amersham Biosciences). Remaining endotoxins were removed using detoxigel columns (Pierce, Rockford, IL).

$(Z_{HER2:342})_2$ was fermented, and the cells were disintegrated by sonication on ice and centrifuged. The supernatant was purified on a cation exchange column SP Sepharose Fast Flow (Pharmacia Biotech, Uppsala, Sweden) and a reverse-phase column RESOURCE RPC 3 mL (Amersham Biosciences). Remaining endotoxins were removed using detoxigel columns (Pierce).

Conjugation and labeling chemistry. ^{125}I-ABD-$(Z_{HER2:342})_2$ was labeled using *p*-iodobenzoate linker according to the procedure described by Orlova et al. (9).

Conjugation of the isothiocyanate derivative of CHX-A″-DTPA to Affibody molecules, both specific ABD-$(Z_{HER2:342})_2$ and nonspecific ABD-$(Z_{abeta})_2$, was done at elevated temperature in alkaline aqueous solution, according to a method previously used (27), using a chelator-to-protein molar ratio of 1:1. Briefly, 333 μL ABD-$(Z_{HER2:342})_2$ (400 μg) was mixed with 16 μL of freshly prepared solution (1 mg/mL) of isothiocyanate-CHX-A″-DTPA (Macrocyclics, Dallas, TX) in 0.07 mol/L sodium borate buffer (pH 9.2). The total volume was adjusted to 500 μL with 0.07 mol/L borate buffer, after which the mixture was vortexed for about 30 s and then incubated overnight at 37°C. After incubation, the reaction mixture was purified on a NAP-5 size exclusion column pre-equilibrated with 1 mol/L ammonium acetate buffer (pH 5.5) containing 5 g/L ascorbic acid. The eluate was vortexed and stored at −20°C before labeling. Nonspecific ABD-fused ABD-$(Z_{abeta})_2$ Affibody molecule and non–ABD-fused $(Z_{HER2:342})_2$ was conjugated with chelator using the same protocol.

To evaluate the efficiency of isothiocyanate-CHX-A″-DTPA coupling to ABD-$(Z_{HER2:342})_2$, two samples were analyzed by high-performance liquid chromatography and online mass spectrometry (HPLC-MS) using an Agilent 1100 HPLC/MSD. The mass spectrometer was equipped with electrospray ionization and single quadropol. A Zorbax 300SB-C18 (4.6 × 150, 3.5 μm; Agilent, Santa Clara, CA) RPC column eluted with water/acetonitrile gradient with 0.1% trifluoroacetic acid was used.

For labeling, a predetermined amount of conjugate in 1 mol/L ammonium acetate buffer (pH 5.5) was de-frozen and mixed with a predetermined amount of ^{177}Lu and incubated at room temperature for 30 to 60 min. A 2-fold molar excess of Affibody molecule over lutetium was used.

For routine quality control of the labeling, ITLC SG (silica gel impregnated glass fiber sheets for instant TLC, Gelman Sciences, Inc., East Hills, NY) eluted with 0.2 mol/L citric acid was used. In this system, radiolabeled Affibody molecules remain at origin, free lutetium migrates with the front of solvent, and ^{177}Lu-CHX-A″-DTPA complex has a R_f of 0.4. Distribution of radioactivity along the instant TLC strips was measured on a Cyclone Storage Phosphor System and analyzed using the OptiQuant image analysis software.

Affinity was measured using Biacore 3000 (Biacore AB, Uppsala, Sweden) with Sensor Chip CM5. HER-2 was immobilized using amine chemistry according to the manufacturer's instructions. To obtain monomeric affinity, surface density of ECD-HER2 was kept low to exclude avid interaction of the conjugate with two receptors simultaneously. Conjugate was injected for 600 s at five concentrations ranging from 15 pmol/L to 6.4 nmol/L. Results were evaluated with BIAevaluation 4.0 (Biacore) using a 1:1 interaction model.

Cell binding and retention studies. The binding specificity of the obtained conjugates was tested on HER2-expressing SKOV-3 ovarian cancer cells according to method described earlier (26). For HER2 saturation, a 1,000-fold excess of nonlabeled Affibody molecule or pertuzumab was used. To evaluate how residualizing properties of label affect the retention, a cellular retention of radioactivity after interrupted incubation with ^{125}I-ABD-$(Z_{HER2:342})_2$ and ^{177}Lu- CHX-A″-DTPA-ABD-$(Z_{HER2:342})_2$ was studied according to the method described by Orlova et al. (9). To assess the chemical form of radioactivity in the medium after 72 h of incubation, medium was passed through size-exclusion NAP-5 columns (0.5 mL from each sample), and radioactivity of fractions was measured.

Comparative biodistribution of $(Z_{HER2:342})_2$ with and without ABD in normal mice. All animal studies were approved by the local Ethics

Committee. To evaluate influence of ABD on biodistribution, ^{177}Lu-CHX-A″-DTPA-$(Z_{HER2:342})_2$ and ^{177}Lu-CHX-A″-DTPA-ABD-$(Z_{HER2:342})_2$ were given s.c. to female NMRI mice (12 weeks; Taconic Europe A/S, Ry, Denmark). At 1 [only $(Z_{HER2:342})_2$], 4, 8, 24, 48, 72, and 168 h after injection, animals were injected with a lethal dose of Ketalar/Rompun and dissected (n = 4 for each time point). Blood, lung, liver, spleen, kidneys, salivary glands, skin, and bone were collected for radioactive measurement. Uptake was calculated and expressed as percent injected activity per gram (% IA/g).

Tumor uptake and biodistribution of ^{177}Lu in SKOV-3 xenograft-bearing nude mice after s.c. injection of ^{177}Lu-CHX-A″-DTPA-ABD-$(Z_{HER2:342})_2$. Female mice (BALB/c *nu/nu*; 10–12 weeks old at arrival; Taconic) were injected with $\sim 10^7$ SKOV-3 cells s.c. in the hind leg 4 weeks before the experiment. Forty mice with SKOV-3 tumor xenografts were randomized into 10 groups (n = 4). Eight groups of mice were injected s.c. with 1 μg ^{177}Lu-CHX-A″-DTPA-ABD-$(Z_{HER2:342})_2$ with activity of 110 kBq in 100 μL PBS and killed 1, 4, 12, 24, 48, 72, 168, and 332 h after injection. For specificity control, the ninth group was pretreated with nonlabeled ABD-$(Z_{HER2:342})_2$ (335 μg, 0.5 mL PBS) 45 min before injection of ^{177}Lu-CHX-A″-DTPA-ABD-$(Z_{HER2:342})_2$ and killed 24 h after injection. To evaluate the level of nonspecific accumulation in tumors, the 10th group was injected s.c. with non–HER2-specific Affibody molecule ^{177}Lu-DTPA-CHX-A″- ABD-$(Z_{abeta})_2$ (1 μg, 110 kBq, 100 μL PBS) and sacrificed 48 h after injection. Blood, lung, liver, spleen, kidneys, salivary glands, skin, and bone were collected for radioactive measurement subsequently expressed as % IA/g. Typical weight of xenografts excised during first 24 h of the study was ~100 mg. At the end of the study, xenograft weight increased to about 250 mg due to tumor growth.

Dosimetry calculations. The organ uptake values from the biodistribution study, noncorrected for physical half-life, were time integrated to obtain the residence time per gram tissue for dosimetry calculations. Integration between time 0 and 332 h was made by the trapezoid method. The two last time points were fitted to a single exponential function, which was used to estimate the residence time from 332 h to infinity. The extrapolated area was less than a few percent in all organs except the liver and the spleen where the value was found to be ~15 %.

Assuming normal distribution, the mean uptake values and their SDs given in Table 1 were used to randomly generate 30 sets of new uptake values. For each data set, the absorbed doses was calculated in the same way as described above. The SD in this data set was used as the error of the calculated absorbed dose in the organs.

In the absorbed dose calculations, S values for ^{177}Lu were obtained from RADAR phantoms (Unit Density Spheres) published on the Internet.[4] The S value for a 1 g sphere (0.0233 mGy/MBq s) was used generally to calculate all organ doses. This simplified dosimetry calculation is motivated by the fact that the low-energy β-particles in the ^{177}Lu decay are locally absorbed, and photons and other penetrating radiations are contributing to a low extent, which means that the cross-talk between different organs in the mouse is negligible.

Gamma-camera imaging. Three mice were injected i.v. with ^{177}Lu-CHX-A″-DTPA-ABD-$(Z_{HER2:342})_2$ (3 MBq, 150 μL PBS) and killed 52 h after injection. Gamma-camera imaging was done at the Department of Nuclear Medicine, Uppsala University Hospital. Static images with a gamma-camera were made with a Millenium VG with 5/8 in. NaI(Tl) crystal (General Electric, Haifa, Israel). The images were acquired during 10 min in 256 × 256 matrix, with a zoom factor of 2.0, and the energy windows were set to 113 ± 10% and 208 ± 10%.

Experimental radionuclide therapy of nonestablished xenografts. The effect of ^{177}Lu-CHX-A″-DTPA-ABD-$(Z_{HER2:342})_2$ on xenografts with high level of HER2 expression was studied using SKOV-3 cells. Female mice (BALB/c *nu/nu*; 10–12 weeks old at arrival; Taconic) were injected with $\sim 10^7$ SKOV-3 cells s.c. on the abdomen. Seven days later, all animals were treated with a single injection of radiolabeled Affibody molecules (20 μg, 1 nmol).

[4] http://www.doseinfo-radar.com/RADARphan.html

^{177}Lu-CHX-A″-DTPA-ABD-$(Z_{HER2:342})_2$ was injected using three different radioactivity levels (mean ± SD): 17.5 ± 0.4 MBq (n = 10), 21.6 ± 0.3 MBq (n = 22), and 29.6 ± 0.3 MBq (n = 10). Moreover, a control group (n = 10) received the same volume of PBS. To investigate if the tumor growth could be influenced by unspecific irradiation due to radiolabeled Affibody molecules circulating in the blood, another control group (n = 10) was injected with 21.4 ± 0.2 MBq ^{177}Lu-CHX-A″-DTPA-ABD-$(Z_{abeta})_2$. The study was terminated 104 days after drug administration.

The presence and size of tumors were assessed twice a week using a slide caliper. Mice were euthanized if body weight loss exceeded 20% or tumors were larger than 1 mL or were ulcerated. Tumors, kidneys, and serum/blood were saved upon termination. Assay of leukocyte counts and serum creatinine concentration as well as histopathologic evaluation of kidneys were carried out in an external laboratory (SVA, Uppsala, Sweden).

To assess the influence of radionuclide therapy using ^{177}Lu-CHX-A″-DTPA-ABD-$(Z_{HER2:342})_2$ on xenografts derived from cells with low level of HER2 expression, a colorectal carcinoma cell line LS174T was used (20, 36). Female mice (BALB/c *nu/nu*; 10–12 weeks old at arrival; Taconic) were injected with 3 × 10^6 LS174T cells s.c. on the abdomen. Animals were treated with a single injection of radiolabeled Affibody molecules (20 μg, 1 nmol) when they had palpable tumors (20–30 μL). Mice were injected with either 22.2 MBq ^{177}Lu-CHX-A″-DTPA-ABD-$(Z_{HER2:342})_2$ (n = 9), 22.3 MBq of non–HER2-specific ^{177}Lu-CHX-A″-DTPA-ABD-$(Z_{abeta})_2$ (n = 8, control), or PBS (n = 9). The presence and size of tumors were assessed as described above, and animals were euthanized if tumors were larger than 1 mL or were ulcerated. The study was terminated 72 days after drug administration.

Statistics. Data on cellular uptake and biodistribution were analyzed by a two-tailed t test using GraphPad Prism (version 4.00 for Windows GraphPad Software, San Diego, CA) to determine any significant differences ($P < 0.05$). Tumor-free survival (i.e., days after drug administration a mouse was alive without tumor) were compared among the groups using log-rank test (GraphPad Prism). Differences in body weight and serum creatinine concentration were tested using Student's unpaired t test (Microsoft Excel).

Results

Production of $(Z_{HER2:342})_2$ and ABD-$(Z_{HER2:342})_2$

The purified proteins were identified and characterized by LC/MS and SDS-PAGE. In both analyses, no contaminants could be detected, and the purity of the proteins was determined from the LC/MS to be >98%. The molecular masses were in agreement with the theoretical values. The final concentration of ABD-$(Z_{HER2:342})_2$ was 1.58 mg/mL and for $(Z_{HER2:342})_2$ 1.14 mg/mL.

Conjugation and Labeling Chemistry

LS/MS showed that on average, 0.91 chelator was coupled per molecule of ABD-$(Z_{HER2:342})_2$. We did not further increase the number of chelator per protein due to the risk of over-modification. According to surface plasmon resonance measurement, a chelator-coupled Affibody molecule retained high affinity both to albumin (K_d of 31 and 8.2 nmol/L to murine and human albumin, respectively) and to the extracellular domain of HER2 (18 pmol/L). Labeling of CHX-A″-DTPA-ABD-$(Z_{HER2:342})_2$ was quick and efficient, providing yield of 88.6 ± 2.0% after 15 min and 96.8 ± 0.6% after 30 min (n = 6), with very little batch-to-batch variation.

Cell Binding and Retention Studies

In agreement with the surface plasmon resonance data, radiolabeled conjugate retained capacity to bind to living HER2-expressing SKOV-3 cells. Presaturation of receptor with an excess of nonlabeled ABD-$(Z_{HER2:342})_2$ caused almost complete blocking of

Table 1. Comparative biodistribution of ^{177}Lu-CHX-A″-DTPA-$(Z_{HER2:342})_2$ and ^{177}Lu-CHX-A″-DTPA-ABD-$(Z_{HER2:342})_2$ in NMRI mice

	1 h	4 h		8 h		24 h	
	$(Z_{HER2:342})_2$	$(Z_{HER2:342})_2$	ABD-$(Z_{HER2:342})_2$	$(Z_{HER2:342})_2$	ABD-$(Z_{HER2:342})_2$	$(Z_{HER2:342})_2$	ABD-$(Z_{HER2:342})_2$
Blood	1.2 ± 0.3	0.059 ± 0.004	5 ± 1	0.027 ± 0.001	8 ± 1	0.023 ± 0.006	7.0 ± 0.8
Lung	1.0 ± 0.2	0.26 ± 0.03	1.5 ± 0.4	0.24 ± 0.05	2 ± 1	0.17 ± 0.02	3.4 ± 0.4
Liver	1.2 ± 0.2	1.5 ± 0.4	1.0 ± 0.3	1.5 ± 0.2	2.0 ± 0.3	1.19 ± 0.04	4.1 ± 0.1
Spleen	0.7 ± 0.2	0.5 ± 0.1	0.6 ± 0.3	0.41 ± 0.08	1.3 ± 0.1	0.31 ± 0.02	2.1 ± 0.2
Kidney	109 ± 7	149 ± 38	5.8 ± 0.6	155 ± 20	9 ± 1	104 ± 11	11 ± 1
Salivary gland	0.6 ± 0.1	0.25 ± 0.06	0.7 ± 0.1	0.24 ± 0.05	1.4 ± 0.3	0.21 ± 0.01	2.1 ± 0.4
Skin	3 ± 3	1 ± 1	1 ± 1	0.58 ± 0.07	6 ± 3	0.3 ± 0.1	5 ± 3
Bone	0.5 ± 0.1	0.3 ± 0.1	0.3 ± 0.2	0.24 ± 0.05	0.7 ± 0.1	0.19 ± 0.05	1.2 ± 0.2

NOTE: Each data point presents an average from four animals ± SD and is expressed as the percentage of injected radioactivity per gram organ or tissue.
Abbreviation: NM, not measurable.

binding (data not shown). An attempt to add a blocking amount of pertuzumab did not reduce binding at all, which indicates that these two targeting proteins bind to different epitopes.

Cellular retention experiments showed much better retention of ^{177}Lu label in comparison with radioiodine one (Fig. 1). This is a strong indication of internalization of the ABD-$(Z_{HER2:342})_2$–based conjugates. Good retention, typical for radiometals, resulted in that 44.1 ± 0.1% of radioactivity was still associated with cells 72 h after medium change. A size-exclusion chromatography showed that only 5% to 10% of lutetium in the medium was bound to high-molecular-weight compounds. This indicates that exocytosis of degraded Affibody molecules is the main route of decrease of cell-associated radioactivity.

Comparative Biodistribution of $(Z_{HER2:342})_2$ with and without ABD in Normal Mice

Results of the comparison of $(Z_{HER2:342})_2$ with or without ABD are presented in Table 1. The residence of $(Z_{HER2:342})_2$ in the blood circulation was prolonged with an increase of the half-life from 0.64 ± 0.2 to 35.8 ± 0.0 h, and radioactivity uptake in kidney was reduced 25-fold in comparison with the peak value for ^{177}Lu-CHX-A″-DTPA-$(Z_{HER2:342})_2$. Low uptake in bone indicated high stability of chelate and confirmed that the chelator was suitable for therapy. The radioactivity concentration in organs and tissues after injection of ^{177}Lu-CHX-A″-DTPA-ABD-$(Z_{HER2:342})_2$ generally followed its kinetics in blood.

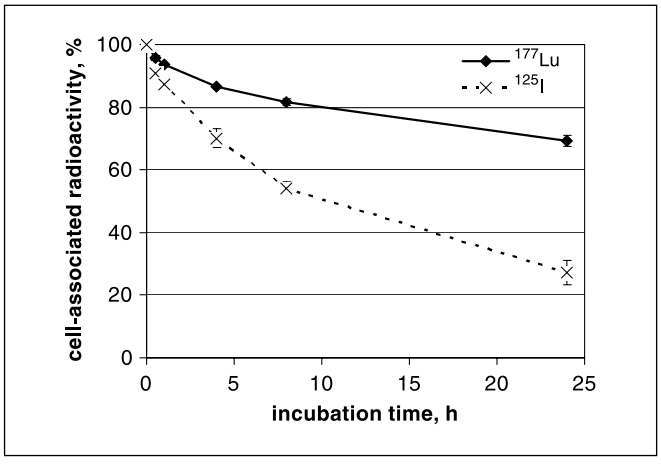

Figure 1. Cell-associated radioactivity as a function of time after interrupted incubation of SKOV-3 cells with ^{177}Lu-CHX-A″-DTPA-ABD-$(Z_{HER2:342})_2$ (*solid line*) and ^{125}I-PIB-ABD-$(Z_{HER2:342})_2$ (*dotted line*). The cell-associated radioactivity at time 0 after the interrupted incubation was considered as 100%. *Points,* mean (n = 3); *bars,* SD. Bars might not be seen because they are smaller than points.

Tumor Uptake and Biodistribution of ^{177}Lu in SKOV-3 Xenograft-Bearing Nude Mice after Subcutaneous Injection of ^{177}Lu-CHX-A″-DTPA-ABD-$(Z_{HER2:342})_2$

Biodistribution and dosimetric data are presented in Table 2. The biodistribution showed high uptake in the tumors after about 24 h after injection. Then, tumor radioactivity concentration exceeded that in blood and kidneys. Concentration in blood and kidneys (highest among healthy tissue) peaked at 12 and 24 h after injection, respectively. Skin uptake was also high, in agreement with abundance of albumin due to relatively large fractional interstitial volume (37). Bone uptake was low, indicating that free ^{177}Lu was neither released when ^{177}Lu-CHX-A″-DTPA-ABD-$(Z_{HER2:342})_2$ was in circulation nor after its degradation in tumor and excretory organs. Radioactivity in normal organs decreased with time, mainly following blood kinetics. Exceptions were liver and spleen, which is probably a sign of internalization of the conjugate.

Importantly, specificity of tumor uptake was shown in two independent experiments (Fig. 2). First, preinjecting large molar excess of nonlabeled ABD-$(Z_{HER2:342})_2$ decreased tumor uptake 24 h after injection from 19 ± 7 to 6.7 ± 0.3% IA/g (P < 0.05), proving saturability of tumor uptake and a receptor-mediated mechanism. There were no statistically significant differences in uptake for other organs with or without pretreatment with nonlabeled ABD-$(Z_{HER2:342})_2$.

In the second experiment, a nonspecific Affibody dimer fused to ABD was injected. A comparison showed significantly lower levels (P < 0.0005) of radioactivity at 48 h not only in the tumor but also in blood. However, the reduction of blood level was only 2-fold, whereas tumor accumulation was 9.6-fold lower. This indicated that accumulation of ^{177}Lu-CHX-A″-DTPA-ABD-$(Z_{HER2:342})_2$

Table 1. Comparative biodistribution of ^{177}Lu-CHX-A″-DTPA-$(Z_{HER2:342})_2$ and ^{177}Lu-CHX-A″-DTPA-ABD-$(Z_{HER2:342})_2$ in NMRI mice (Cont'd)

48 h		72 h		168 h	
$(Z_{HER2:342})_2$	ABD-$(Z_{HER2:342})_2$	$(Z_{HER2:342})_2$	ABD-$(Z_{HER2:342})_2$	$(Z_{HER2:342})_2$	ABD-$(Z_{HER2:342})_2$
0.006 ± 0.001	4.0 ± 0.9	0.007 ± 0.002	3.2 ± 0.3	NM	0.6 ± 0.2
0.10 ± 0.04	2.3 ± 0.5	0.06 ± 0.02	2.2 ± 0.2	NM	0.80 ± 0.07
0.8 ± 0.1	4.3 ± 0.9	0.6 ± 0.1	5 ± 1	0.47 ± 0.08	3.8 ± 0.5
0.3 ± 0.1	1.8 ± 0.3	0.17 ± 0.05	2.0 ± 0.1	0.14 ± 0.04	1.7 ± 0.2
54 ± 7	10 ± 1	34 ± 11	9 ± 1	8 ± 2	2.7 ± 0.8
0.11 ± 0.04	1.7 ± 0.4	0.09 ± 0.01	1.74 ± 0.08	0.07 ± 0.01	0.9 ± 0.2
0.5 ± 0.2	3 ± 2	0.6 ± 0.4	2.6 ± 0.8	0.13 ± 0.04	1.1 ± 0.3
0.1 ± 0.1	0.9 ± 0.2	0.13 ± 0.08	0.8 ± 0.2	0.20 ± 0.07	0.6 ± 0.2

in tumor depends on its interaction with HER2-receptors and not on unspecific trapping of proteins in tumor interstitium as a consequence of higher fractional interstitial volume of tumor tissue. The lower blood concentration of nonspecific Affibody may suggest that some part of the radiolabeled ^{177}Lu-CHX-A″-DTPA-ABD-$(Z_{HER2:342})_2$ dissociated continuously from the receptors, was drained from the tumors, and then re-entered the blood circulation, whereas such a depot did not exist for the nonspecific Affibody ^{177}Lu-CHX-A″-DTPA-ABD-$(Z_{abeta})_2$.

Gamma-Camera Imaging

Gamma-camera imaging (Fig. 3) confirmed good tumor targeting properties of ^{177}Lu-CHX-A″-DTPA-ABD-$(Z_{HER2:342})_2$. It was seen that already 52 h after injection, tumor xenografts were the only sites of prominent accumulation of radioactivity. Elevated (in comparison with rest of the animal) radioactivity accumulation was also seen in the abdominal area. However, there was no clear visualization of kidneys, which has been characteristic for previously obtained gamma-camera images using radiometal-labeled Affibody molecules that were not fused with ABD.

Experimental Radionuclide Therapy of Microxenografts

SKOV-3 (high HER2 expression) xenografts. For vehicle-treated animals (n = 10), tumors appeared in seven animals 36 to 62 days (median, 43 days) after injection. Mice with tumors were euthanized 67 to 104 days (median, 67 days) after administration due to tumor growth.

Among mice given 21.4 MBq (n = 10) of nonspecific ^{177}Lu-CHX-A″-DTPA-ABD-$(Z_{abeta})_2$, tumors appeared in six animals 18 to 85 days (median, 43 days) after administration. Compared with vehicle-treated mice, there was no statistical significant difference.

Among mice given 17.4 (n = 10) and 21.6 MBq (n = 22) ^{177}Lu-CHX-A″-DTPA-ABD-$(Z_{HER2:342})_2$, tumors could not be detected throughout the study period. Thus, tumor-free survival was significantly different (17.4 MBq, $P < 0.05$; 21.6 MBq, $P < 0.001$) compared with mice treated with 21.4 MBq ^{177}Lu-CHX-A″-DTPA-ABD-$(Z_{abeta})_2$. Except for two animals that had to be euthanized days 1 and 18 after drug administration due to loss of weight, all animals survived tumor-free up to study termination (Fig. 4*A*).

Table 2. Biodistribution and dosimetry of ^{177}Lu-CHX-A″-DTPA-ABD-$(Z_{HER2:342})_2$ in BALB/c *nu/nu* mice bearing HER2-expressing SKOV-3 xenografts

	% IA/g								Gy/MBq
	1 h	4 h	12 h	24 h	48 h	72 h	168 h	332 h	
Blood	0.9 ± 0.3	7 ± 2	13.4 ± 0.2	9.7 ± 0.5	5.5 ± 0.8	3.5 ± 0.6	0.43 ± 0.07	0.007 ± 0.004	0.51 ± 0.3
Tumor	0.13 ± 0.04	1.9 ± 0.4	7 ± 4	19 ± 7	26 ± 4	21 ± 6	9 ± 1	1.8 ± 0.2	2.1 ± 0.2
Heart	0.13 ± 0.09	1.5 ± 0.3	3.8 ± 0.2	3.2 ± 0.4	2.5 ± 0.3	1.8 ± 0.5	0.86 ± 0.03	0.44 ± 0.03	0.25 ± 0.02
Lung	0.3 ± 0.1	2.4 ± 0.4	5.7 ± 0.1	4.7 ± 0.3	3.5 ± 0.5	2.8 ± 0.3	0.87 ± 0.03	0.3 ± 0.2	0.33 ± 0.01
Liver	0.22 ± 0.09	1.4 ± 0.4	3.9 ± 0.3	4.8 ± 0.3	5.7 ± 0.6	5.3 ± 0.5	4.1 ± 0.5	3.0 ± 0.3	0.76 ± 0.03
Spleen	0.18 ± 0.04	1.0 ± 0.2	3.0 ± 0.2	2.9 ± 0.2	3.8 ± 0.4	3.6 ± 0.7	2.6 ± 0.2	2.3 ± 0.2	0.53 ± 0.4
Pancreas	0.14 ± 0.08	0.48 ± 0.02	1.6 ± 0.2	1.6 ± 0.2	1.3 ± 0.2	0.9 ± 0.1	0.47 ± 0.07	0.18 ± 0.02	0.12 ± 0.01
Stomach	0.09 ± 0.03	0.47 ± 0.09	1.60 ± 0.09	1.3 ± 0.2	1.1 ± 0.1	0.78 ± 0.05	0.26 ± 0.05	0.08 ± 0.08	0.097 ± 0.003
Intestine	0.12 ± 0.04	0.8 ± 0.2	1.5 ± 0.7	1.5 ± 0.2	1.5 ± 0.2	0.94 ± 0.06	0.31 ± 0.04	0.03 ± 0.03	0.11 ± 0.005
Kidney	3.3 ± 0.9	7 ± 2	13.4 ± 0.8	15 ± 2	15.9 ± 0.8	13 ± 1	6.1 ± 0.4	2.0 ± 0.2	1.49 ± 0.07
Salivary gland	0.10 ± 0.01	1.0 ± 0.3	4.21 ± 0.10	2.9 ± 0.4	3.2 ± 0.3	2.7 ± 0.4	1.74 ± 0.07	1.2 ± 0.3	0.38 ± 0.02
Skin	5 ± 3	7 ± 3	8 ± 2	7 ± 1	6 ± 1	4 ± 1	2.0 ± 0.4	1.0 ± 0.3	0.57 ± 0.05
Muscle	0.6 ± 0.5	0.7 ± 0.3	1.31 ± 0.07	1.3 ± 0.3	1.0 ± 0.3	0.60 ± 0.05	0.32 ± 0.06	0.12 ± 0.06	0.09 ± 0.001
Bone	0.11 ± 0.05	0.51 ± 0.01	1.5 ± 0.3	1.4 ± 0.2	1.8 ± 0.6	1.1 ± 0.8	1.2 ± 0.4	0.9 ± 0.7	0.21 ± 0.05
Brain	0.03 ± 0.03	0.15 ± 0.04	0.29 ± 0.01	0.23 ± 0.01	0.13 ± 0.02	0.4 ± 0.4	0.016 ± 0.004	Not detected	0.02 ± 0.01

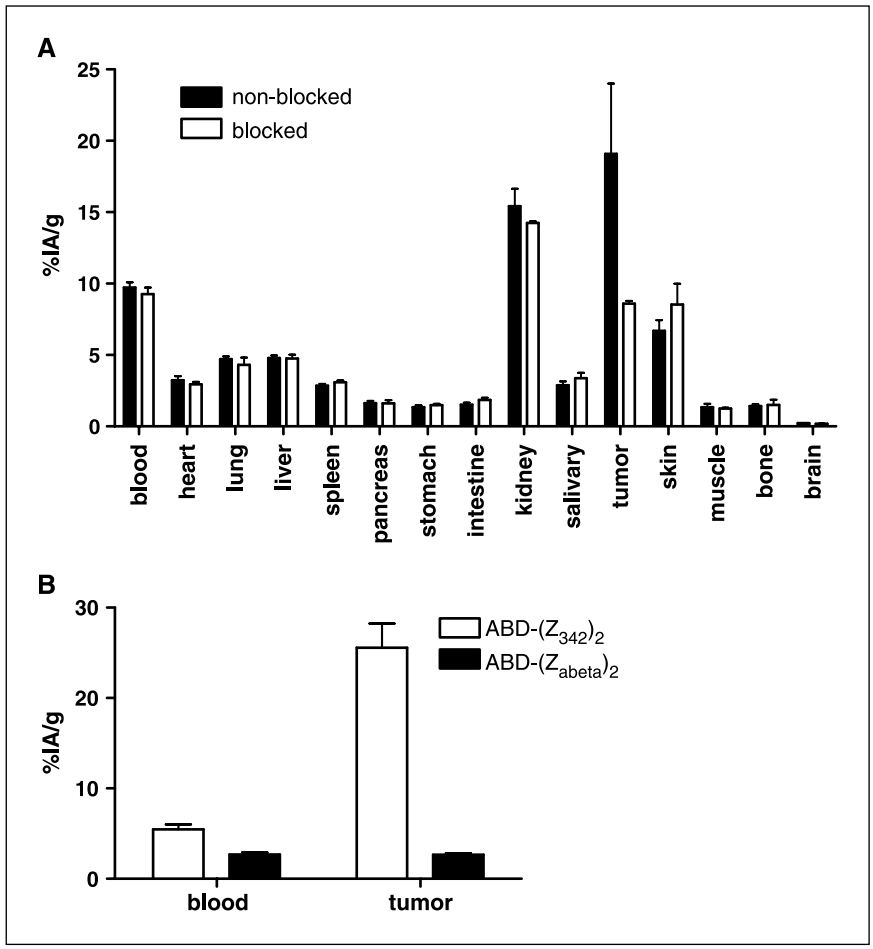

Figure 2. Specificity of ^{177}Lu-CHX-A″-DTPA-ABD-$(Z_{HER2:342})_2$ uptake in HER2-expressing xenografts. *A,* one group of animals was preinjected with 335 μg of nonlabeled ABD-$(Z_{HER2:342})_2$ to saturate HER2 receptors 45 min before injection of radiolabeled conjugate. All animals were injected with 20 μg ^{177}Lu-CHX-A″-DTPA-ABD-$(Z_{HER2:342})_2$ and dissected 24 h after injection. Significant difference ($P < 0.05$) between blocked and nonblocked groups was only observed in tumors. *Columns,* mean ($n = 4$); *bars,* SD. *B,* one group of animals was injected with 20 μg of nonspecific ^{177}Lu-CHX-A″-DTPA-ABD-$(Z_{abeta})_2$ Affibody molecule and dissected 48 h after injection. Significant difference ($P < 0.05$) between specific and nonspecific Affibody molecules were observed both in blood and tumors. *Columns,* mean ($n = 4$); *bars,* SD.

Animal weight was not different between the groups on the day of administration. Following drug administration, body weight was not significantly different among the groups, up to 78 days after administration, except for mice given 29.6 MBq. Thereafter, body weight in vehicle-treated mice was significantly lower compared with mice given 17.4 to 21.6 MBq ^{177}Lu-CHX-A″-DTPA-ABD-$(Z_{HER2:342})_2$. The decrease of body weight in this group was due to tumor development.

Mice given 29.6 MBq ($n = 12$) had to be sacrificed 8 to 18 days after drug administration due to illness and decline in body weight. In blood analyzed from three of these mice, no leukocytes were observed. In vehicle-treated mice, blood leukocyte counts were 3.0 to 4.2 $\times$ 10^9 cells per mL ($n = 4$), close to that found in normal mice. This indicates that myelotoxicity was dose limiting.

Serum creatinine concentration in treated mice sacrificed at the study end (21.6 MBq, $n = 9$, 26–33 μmol/L) or 6 months after drug administration (17.5 MBq, $n = 4$, 17–27 μmol/L; 21.6 MBq, $n = 2$, 25–31 μmol/L) was not significantly different compared with vehicle-treated mice ($n = 3$, 23–24 μmol/L), except for one mouse given 17.4 MBq (94 μmol/L). Histopathology examinations of kidneys in mice given 17.4 MBq and sacrificed 3 weeks later revealed no pathologic changes.

LS174T (low HER2 expression) xenografts. The therapy study was also done in the LS174T model, which served as a model for tumors with low HER2 expression. Mice that were treated with 22.2 MBq of ^{177}Lu-CHX-A″-DTPA-ABD-$(Z_{HER2:342})_2$ had a statistically significant prolonged survival compared with mice treated with 22.3 MBq of the non–HER2-specific control Affibody molecule ^{177}Lu-CHX-A″-DTPA-ABD-$(Z_{abeta})_2$ ($P = 0.006$) or vehicle ($P = 0.001$; Fig. 4*B*). Although the initial reduction in tumor growth was apparent for the treated group, tumor formation was not prevented in this study. The main cause of animal euthanasia in the treatment group was tumor ulceration rather than overgrowth. No increase in serum creatinine concentration was observed ($n = 6$), and body weight was not different among the groups.

Discussion

Design of tumor targeting radiopharmaceuticals is a complex problem, which requires a careful consideration of a number of factors, such as nature of the tumor-associated target, including cellular processing of target-targeting agent complex, the physical properties of the radionuclide, labeling chemistry, and biodistribution properties of the targeting agents. This study is concentrated mainly on the biodistribution aspect. Radioimmunotherapy studies have mainly used IgG as a targeting vector (38). Long circulation time provides high tumor accumulation of slowly extravasating bulky immunoglobulins but, at the same time, causes unacceptably high doses to bone marrow. This can be avoided by increasing the tumor to blood ratio by improving

extravasation and tumor penetration, or reducing blood residence time, or combining both approaches. Several alternative methodologies aiming to minimize residence time of radioactivity in circulation and/or improving tumor localization are under evaluation, such as different ways of pre-targeting (39), extracorporeal filtration of radiolabeled antibodies (40), avidin chase of biotinylated antibodies (41), the engineering of smaller antibody-base constructs (5) or the use of peptide receptor ligands (7) with fast blood kinetics. We previously developed the $Z_{HER2:342}$ Affibody molecule with very rapid (within 1 h) tumor localization and elimination, resulting in high tumor/nontumor ratios. However, radioactive dose to kidneys was unacceptably high for both nonresidualizing iodine (9) and residualizing indium (27) labels. $Z_{HER2:342}$, being a small protein, is freely filtered through glomerular membranes and subsequently reabsorbed into kidney parenchyma. In this study, we aimed for a reduction in renal accumulation by noncovalent binding to albumin preventing glomerular filtration.

A monovalent and divalent form of $Z_{HER2:342}$ were fused to ABD. We found that the monovalent form had a decrease in binding affinity to HER2, both in biosensor measurements (20-fold lower) and in experiments with living HER2-expressing cells (data not shown). A possible reason could be sterical hindrance of ABD in binding of the $Z_{HER2:342}$, as the on-rate but not the off-rate was affected. The use of high-affinity targeting agents for therapy is controversial. Adams et al. (23) have earlier observed that increase of affinity of scFv beyond K_d of 1 nmol/L may not increase quantitative retention of radioiodine label in tumors and can result in an nonhomogenous uptake, predominantly around blood vessels. However, modeling studies (42, 43) on targeting β-emitting nuclides, as in our case, suggest that the highest affinity provides the highest dose to the tumor. Our earlier results with non–ABD-fused anti-HER2 Affibody molecules showed increase of tumor localization with increase of affinity (9). For this reason, a high-affinity divalent form was selected.

In vitro analysis confirmed that both ^{125}I-PIB- ABD-$(Z_{HER2:342})_2$ and ^{177}Lu-CHX-A″-DTPA-ABD-$(Z_{HER2:342})_2$ conjugates retained capacity to bind to HER2-expressing cells *in vitro*. However, cellular retention experiments showed appreciably better retention of the residualizing metal label (^{177}Lu) in comparison with the nonresidualizing halogen (^{125}I). Because poor intracellular retention reduces both the radioactivity accumulation in tumors and the specificity of targeting (43, 44), the ^{177}Lu-labeled conjugate was selected for further investigations. Interestingly, we have found that ^{177}Lu-CHX-A″-DTPA-ABD-$(Z_{HER2:342})_2$ binds to a different epitope than pertuzumab. Together with our earlier finding that $Z_{HER2:342}$ does not compete with trastuzumab for binding (8), this opens an opportunity to combine treatments.

In vivo comparison with the non–ABD-fused ^{177}Lu-CHX-A″-DTPA $(Z_{HER2:342})_2$ clearly showed the altered biodistribution as a consequence of fusion with ABD. The effect was most apparent for the blood clearance rate and kidney uptake. Such an effect can only be explained by binding of ^{177}Lu-CHX-A″-DTPA-ABD-$(Z_{HER2:342})_2$ to albumin.

The biodistribution study in xenograft-bearing mice showed the capacity of ^{177}Lu-CHX-A″-DTPA-ABD-$(Z_{HER2:342})_2$ to accumulate in HER2 expressing tumors. Importantly, the tumor uptake was receptor specific, as shown in control experiments that included (*a*) partial saturation of receptors *in vivo* and (*b*) the use of an unspecific Affibody molecule dimer fused with ABD.

It would be interesting to compare ^{177}Lu-CHX-A″-DTPA-ABD-$(Z_{HER2:342})_2$ with other HER2-targeting molecules, which have been described in the literature. A quantitative comparison is complicated because of the large variation in tumor models and mouse strains. However, some qualitative conclusions can be done. Although smaller antibody-fragment based conjugates provide good tumor-to-blood ratios, the use of radiometal-labeled Fab and $(Fab')_2$, fragments of trastuzumab (45, 46), or anti-HER2 diabodies (47) and minibodies (22) caused much higher accumulation of radioactivity in kidneys than in tumors. In

Figure 3. Imaging of distribution of ^{177}Lu-CHX-A″-DTPA-ABD-$(Z_{HER2:342})_2$ in BALB/c *nu/nu* mice bearing HER2-expressing SKOV-3 xenografts. Planar gamma-camera images were acquired 52 h after administration of ^{177}Lu-CHX-A″-DTPA-ABD-$(Z_{HER2:342})_2$. Preferential accumulation of ^{177}Lu in tumors (*right femur*) was clearly visualized.

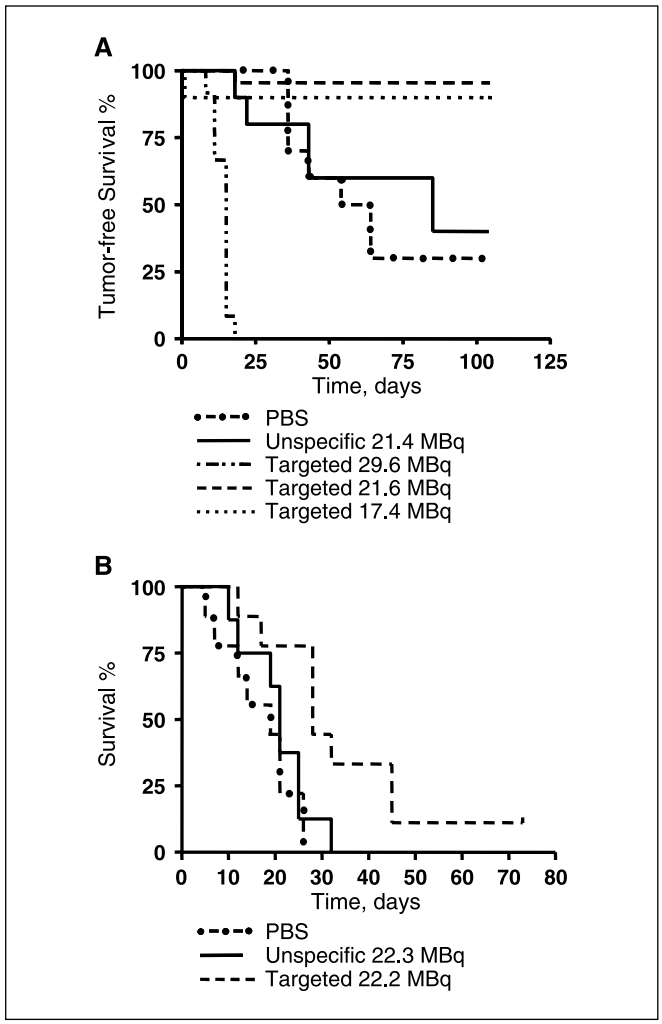

Figure 4. *A,* tumor-free survival of BALB/c *nu/nu* mice with small, established s.c. SKOV-3 tumors versus time. Animals were treated with a single injection of ^{177}Lu-CHX-A″-DTPA-ABD-$(Z_{HER2:342})_2$ (17.4, 21.6, or 29.6 MBq). Animals in control groups were treated either with PBS or with 21.4 MBq of nonspecific ^{177}Lu-CHX-A″-DTPA-ABD-$(Z_{abeta})_2$. *B,* survival until euthanasia criteria of BALB/c *nu/nu* mice with s.c. LS174T tumors versus time. Animals were treated with a single injection of ^{177}Lu-CHX-A″-DTPA-ABD-$(Z_{HER2:342})_2$ (22.2 MBq). Animals in control groups were treated either with PBS or with 22.3 MBq of nonspecific ^{177}Lu-CHX-A″-DTPA-ABD-$(Z_{abeta})_2$.

contrast, blood kinetics of ^{177}Lu-CHX-A″-DTPA-ABD-$(Z_{HER2:342})_2$ resembles the behavior of intact IgG (19–21), with the exception that the renal accumulation is somewhat elevated in comparison with IgG. This is most likely due to a small free fraction that is dissociated from albumin and filtrated through the glomerular membranes. It should be noted that the conjugate has higher affinity to human albumin than to murine albumin, indicating that the free low-molecular-weight fraction should be smaller in humans and thus leading to further reduced renal uptake.

Because our ultimate goal was to investigate methods for therapy of minimal residual disease, our therapeutic model was based on small, established, but not palpable, microxenografts. In this experimental setting, our conjugate had a pronounced therapeutic effect. Administration of 17.4 or 21.6 MBq ^{177}Lu-CHX-A″-DTPA-ABD-$(Z_{HER2:342})_2$ in animals bearing SKOV-3 xenografts with high level of HER2 expression resulted in the complete absence of tumor formation. In contrast, 7 of 10 control mice, injected with PBS, developed tumors. An injection of 21.4 MBq of ^{177}Lu attached to a nonspecific CHX-A″-DTPA-ABD-$(Z_{abeta})_2$ with the same blood kinetics as the targeted molecule did not significantly increase tumor-free survival. This clearly shows that tumor prevention was dependent on specific targeting.

Recently, experimental therapy of nonestablished SKOV-3 xenografts was done using a ^{177}Lu-labeled anti-HER2 antibody pertuzumab (48). The same chelator (CHX-A″-DTPA) was used in that study, and the study protocol was similar to the protocol used in the present study. It was found that both the residence time in blood and tumor uptake were higher for the antibody, whereas kidney uptake was appreciably lower than that for ^{177}Lu-CHX-A″-DTPA-ABD-$(Z_{HER2:342})_2$. According to calculations based on biodistribution in mice bearing macroscopic xenografts, treatment with 7 MBq ^{177}Lu-CHX-A″-DTPA-pertuzumab delivered approximately the same dose to blood as 21.6 MBq ^{177}Lu-CHX-A″-DTPA-ABD-$(Z_{HER2:342})_2$ in this study, but the dose on the tumor was somewhat higher: 50 Gy for the antibody versus 45 Gy for the Affibody molecule–based conjugate. In the case of ^{177}Lu- CHX-A″-DTPA-pertuzumab, a significant increase of survival was achieved in the treatment groups, but in contrast to our current study, tumor formation was not prevented. One possible explanation could be different dose distribution pattern within the xenograft. The tumor cell clump had a diameter of 2 to 3 mm at the time of the treatment. Hypothesizing that pertuzumab due to its size has lower penetration efficiency than the ABD-$(Z_{HER2:342})_2$ molecule, the antibody would stay more localized close to the rim of the tumor (especially if the tumor has not yet become well vascularized). In this case, a cross-fire of low-energy β-particles of ^{177}Lu (mean range, 0.67 mm) would be insufficient to completely eradicate radioresistant hypoxic cells in the middle of the clump. The smaller complex of ^{177}Lu-CHX-A″-DTPA-ABD-$(Z_{HER2:342})_2$ with albumin and particularly the locally released free fraction of ^{177}Lu-CHX-A″-DTPA-ABD-$(Z_{HER2:342})_2$ might penetrate deeper into the tumor and thus provide a more efficient cross-fire effect.

To evaluate the influence of HER2 expression level on the therapy outcome (Fig. 4*B*), we selected LS174T as a model of a tumor with low HER2 expression (49). A lower therapeutic effect could be expected in this case, as there would be fewer receptors per cell that could be targeted by the radiolabeled conjugate. This experiment showed prolonged survival in the case of specific radiolabeled conjugate. However, the tumor formation was not prevented completely. The results of this study imply that careful patient selection is a prerequisite for targeting radionuclide therapy, because only patients with high target expression are expected to get a maximum benefit from such treatment.

In this study, a radioactivity dose sufficient to prevent formation of xenografts with high HER2 expression (up to 21.6 MBq) had no negative effect on the kidneys, assessed by renal histopathology and function (serum creatinine concentration). Our observation is consistent with the literature data. For example, Behr et al. have found in a comprehensive study on renal toxicity due to radionuclide therapy that at renal doses of 40 Gy and even 66 Gy, "no renal toxicity was observed" in a murine model (50). The authors found that acute renal toxicity, with acute nephritis-like picture, was observed at doses above 100 Gy the first weeks after treatment, whereas after more than 5 weeks, and lower doses (about 80 Gy), renal damages in mice resembled chronic radiation

nephrosis. The renal dose for mice treated with 22 MBq in our study was 30 Gy. For comparison, studies on treatment of SKOV-3 using C6.5 diabodies showed a high renal accumulation (47). Therein, 300 μCi (11.1) MBq ^{90}Y impressively reduced growth of established tumors, but already 196 μCi (7.2 MBq) ^{90}Y resulted in functional renal damages manifested by high serum creatinine concentration.

The single administration of 29.6 MBq ^{177}Lu ABD-$(Z_{HER2:342})_2$ resulted in overall mortality within 18 days due to bone marrow toxicity. Albumin-binding affinity, although effective in reducing renal toxicity, increased the exposure to blood and bone marrow. However, a potential advantage of the use of reversible binding to albumin is that it opens for the possibility of fine tuning the drug pharmacokinetics by modifying its affinity to albumin (34). For example, to improve the therapeutic safety window, albumin-binding affinity may be decreased to reduce exposure to bone marrow, while increasing renal exposure within the region of safety.

Conceivably, such an approach could be used not only for targeted radionuclide therapy but also in other occasions where tailoring of the blood plasma half-life of a drug is desired.

Taken together, our results show that fusion with ABD may improve the *in vivo* biodistribution of small tumor-targeting peptides intended for radiotherapy. This modification renders ^{177}Lu-CHX-A″-DTPA-ABD-$(Z_{HER2:342})_2$ a promising candidate for treatment of micrometastases of HER2-expressing malignant tumors.

Acknowledgments

Received 5/3/2006; revised 10/25/2006; accepted 1/9/2007.

Grant support: Swedish Cancer Society and Swedish Governmental Agency for Innovation Systems (VINNOVA).

The costs of publication of this article were defrayed in part by the payment of page charges. This article must therefore be hereby marked *advertisement* in accordance with 18 U.S.C. Section 1734 solely to indicate this fact.

We thank Veronika Eriksson, Lena Israelsson, Ylva Lindman, and the staff of the animal facility at Rudbeck Laboratory for technical assistance and Dr. Lars Abrahmsén (Affibody AB) for comments on the article.

References

1. Volkert WA, Hoffman TJ. Therapeutic radiopharmaceuticals. Chem Rev 1999;99:2269–92.
2. Witzig TE, Gordon LI, Cabanillas F, et al. Randomized controlled trial of yttrium-90-labeled ibritumomab tiuxetan radioimmunotherapy versus rituximab immunotherapy for patients with relapsed or refractory low-grade, follicular, or transformed B-cell non-Hodgkin's lymphoma. J Clin Oncol 2002;20:2453–63.
3. Davis T. Long-term results of a randomized trial comparing tositumomab and iodine-131 Tositumomab (BEXXAR) with tositumomab alone in patients with relapsed or refractory low grade (LG) or transformed low grade (T-LG) non-Hodgkin's lymphoma (NHL). Blood 2003;102:405–6.
4. Goldenberg DM. Targeted therapy of cancer with radiolabeled antibodies. J Nucl Med 2002;43:693–713.
5. Batra SK, Jain M, Wittel UA, Chauhan SC, Colcher D. Pharmacokinetics and biodistribution of genetically engineered antibodies. Curr Opin Biotechnol 2002;13:603–8.
6. Jhanwar YS, Divgi C. Current status of therapy of solid tumors. J Nucl Med 2005;46:141–50.
7. Heppeler A, Froidevaux S, Eberle AN, Maecke HR. Receptor targeting for tumor localisation and therapy with radiopeptides. Curr Med Chem 2000;7:971–94.
8. Wikman M, Steffen AC, Gunnieriusson E, et al. Selection and characterisation of HER2/*neu*-binding affibody ligands. Protein Eng Des Sel 2004;17:455–62.
9. Orlova A, Magnusson M, Eriksson T, et al. Tumor imaging using a picomolar affinity HER2 binding Affibody molecule. Cancer Res 2006;66:4339–48.
10. Nord K, Gunneriusson E, Ringdahl J, Stahl S, Uhlen M, Nygren PA. Binding proteins selected from combinatorial libraries of an alpha-helical bacterial receptor domain. Nat Biotechnol 1997;15:772–7.
11. Ronnmark J, Gronlund H, Uhlen M, Nygren PA. Human immunoglobulin A (IgA)-specific ligands from combinatorial engineering of protein A. Eur J Biochem 2002;269:2647–55.
12. Aunoble B, Sanches R, Didier E, Bignon YJ. Major oncogenes and tumor suppressor genes involved in epithelial ovarian cancer [review]. Int J Oncol 2000;16:567–76.
13. Carlsson J, Nordgren H, Sjostrom J, et al. HER2 expression in breast cancer primary tumours and corresponding metastases. Original data and literature review. Br J Cancer 2004;90:2344–8.
14. Gardmark T, Wester K, de la Torre M, Carlsson J, Malmstrom PU. Analysis of HER2 expression in primary urinary bladder carcinoma and corresponding metastases. BJU Int 2005;95:982–6.
15. Piccart-Gebhart MJ, Procter M, Leyland-Jones B, et al. Trastuzumab after adjuvant chemotherapy in HER2-positive breast cancer. N Engl J Med 2005;353:1659–72.
16. Konecny GE, Pegram MD, Venkatesan N, et al. Activity of the dual kinase inhibitor lapatinib (GW572016) against HER-2-overexpressing and trastuzumab-treated breast cancer cells. Cancer Res 2006;66:1630–9.
17. Baxevanis CN, Sotiriadou NN, Gritzapis AD, et al. Immunogenic HER-2/*neu* peptides as tumor vaccines. Cancer Immunol Immunother 2006;55:85–95.
18. DeNardo SJ. Radioimmunodetection and therapy of breast cancer. Semin Nucl Med 2005;35:143–51.
19. Tsai SW, Sun Y, Williams LE, Raubitschek AA, Wu AM, Shively JE. Biodistribution and radioimmunotherapy of human breast cancer xenografts with radiometal-labeled DOTA conjugated anti-HER2/*neu* antibody 4D5. Bioconjug Chem 2000;11:327–34.
20. Garmestani K, Milenic DE, Plascjak PS, Brechbiel MW. A new and convenient method for purification of ^{86}Y using a Sr(II) selective resin and comparison of biodistribution of ^{86}Y and ^{111}In labeled Herceptin. Nucl Med Biol 2002;29:599–606.
21. Persson M, Tolmachev V, Andersson K, Gedda L, Sandström M, Carlsson J. [^{177}Lu]pertuzumab. Experimental studies on targeting of HER-2 positive tumour cells. Eur J Nucl Med Mol Imaging 2005;32:1457–62.
22. Olafsen T, Tan GJ, Cheung CW, et al. Characterization of engineered anti-p185HER-2 (scFv-CH3)2 antibody fragments (minibodies) for tumor targeting. Protein Eng Des Sel 2004;17:315–23.
23. Adams GP, Schier R, McCall AM, et al. High affinity restricts the localization and tumor penetration of single-chain fv antibody molecules. Cancer Res 2001;61:4750–5.
24. Steffen AC, Orlova A, Wikman M, et al. Affibody mediated tumor targeting of HER-2 expressing xenografts in mice. Eur J Nucl Med Mol Imaging 2006;33:631–8.
25. Mume E, Orlova A, Larsson B, et al. Evaluation of ((4-hydroxyphenyl)ethyl)maleimide for site-specific radiobromination of anti-HER2 affibody. Bioconjug Chem 2005;16:1547–55.
26. Orlova A, Nilsson F, Wikman M, Ståhl S, Carlsson J, Tolmachev V. Comparative *in vivo* evaluation of iodine and technetium labels on anti-HER2 affibody for single-photon imaging of HER2 expression in tumors. J Nucl Med 2006;47:512–9.
27. Tolmachev V, Nilsson FY, Widström C, et al. ^{111}In-benzyl-DTPA-ZHER2:342, an Affibody-based conjugate for *in vivo* imaging of HER2 expression in malignant tumors. J Nucl Med 2006;47:846–53.
28. Peters T, Jr. Serum albumin. Adv Protein Chem 1985;37:161–245.
29. Yeh P, Landais D, Lemaitre M, et al. Design of yeast-secreted albumin derivatives for human therapy: biological and antiviral properties of a serum albumin-CD4 genetic conjugate. Proc Natl Acad Sci U S A 1992;89:1904–8.
30. Syed S, Schuyler PD, Kulczycky M, Sheffield WP. Potent antithrombin activity and delayed clearance from the circulation characterize recombinant hirudin genetically fused to albumin. Blood 1997;89:3243–52.
31. Osborn BL, Sekut L, Corcoran M, et al. Albutropin: a growth hormone-albumin fusion with improved pharmacokinetics and pharmacodynamics in rats and monkeys. Eur J Pharmacol 2002;456:149–58.
32. Makrides SC, Nygren PA, Andrews B, et al. Extended *in vivo* half-life of human soluble complement receptor type 1 fused to a serum albumin-binding receptor. J Pharmacol Exp Ther 1996;277:534–42.
33. Dennis MS, Zhang M, Meng YG, et al. Albumin binding as a general strategy for improving the pharmacokinetics of proteins. J Biol Chem 2002;277:35035–43.
34. Linhult M, Binz HK, Uhlen M, Hober S. Mutational analysis of the interaction between albumin-binding domain from streptococcal protein G and human serum albumin. Protein Sci 2002;11:206–13.
35. Milenic DE, Brady ED, Brechbiel MW. Antibody-targeted radiation cancer therapy. Nat Rev Drug Discov 2004;3:488–99.
36. Lundberg E, Höidén-Guthenberg I, Larsson B, Uhlén M, Gräslund T. Site-specifically conjugated anti-HER2 Affibody molecules as one-step reagents for target expression analyses on cells and xenograft samples. J Immunol Methods 2007;319:53–63.
37. Levitt DG. The pharmacokinetics of the interstitial space in humans. BMC Clin Pharmacol 2003;3:3.
38. Sharkey RM, Goldenberg DM. Advances in radioimmunotherapy in the age of molecular engineering and pretargeting. Cancer Invest 2006;24:82–97.
39. Paganelli G, Magnani P, Zito F, et al. Three-step monoclonal antibody tumor targeting in carcinoembryonic antigen-positive patients. Cancer Res 1991;51:5960–6.
40. Wang Z, Garkavij M, Tennvall JG, Ohlsson T, Strand SE, Sjogren HO. Application of extracorporeal immunoadsorption to reduce circulating blood radioactivity after intraperitoneal administration of indium-111-HMFGl-biotin. Cancer 2002;94:1287–92.
41. Kobayashi H, Sakahara H, Hosono M, et al. Improved clearance of radiolabeled biotinylated monoclonal antibody following the infusion of avidin as a "chase" without decreased accumulation in the target tumor. J Nucl Med 1994;35:1677–84.
42. Fujimori K, Covell DG, Fletcher JE, Weinstein JN. A modeling analysis of monoclonal antibody percolation through tumors: a binding-site barrier. J Nucl Med 1990;31:1191–8.

43. Baxter LT, Jain RK. Transport of fluid and macromolecules in tumors. III. Role of binding and metabolism. Microvasc Res 1991;41:5–23.
44. Tolmachev V, Orlova A, Lundqvist H. Approaches to improvement of cellular retention of radiohalogen labels delivered by internalizing tumor targeting proteins and peptides. Curr Med Chem 2003;10:2447–60.
45. Tang Y, Wang J, Scollard DA, et al. Imaging of HER2/*neu*-positive BT-474 human breast cancer xenografts in athymic mice using ^{111}In-trastuzumab (Herceptin) Fab fragments. Nucl Med Biol 2005;32:51–8.
46. Smith-Jones PM, Solit DB, Akhurst T, et al. Imaging the pharmacodynamics of HER2 degradation in response to Hsp90 inhibitors. Nat Biotechnol 2004;22:701–6.
47. Adams GP, Shaller CC, Dadachova E, et al. A single treatment of yttrium-90-labeled CHX-A″-C6.5 diabody inhibits the growth of established human tumor xenografts in immunodeficient mice. Cancer Res 2004;64:6200–6.
48. Persson M, Gedda L, Lundqvist H, et al. [^{177}Lu]pertuzumab. Experimental therapy of HER-2 expressing xenografts. Cancer Res 2007;67:326–31.
49. Milenic DE, Garmestani K, Brady ED, et al. Targeting of HER2 antigen for the treatment of disseminated peritoneal disease. Clin Cancer Res 2004;10:7834–41.
50. Behr TM, Goldenberg DM, Becker W. Reducing the renal uptake of radiolabeled antibody fragments and peptides for diagnosis and therapy: present status, future prospects and limitations. Eur J Nucl Med 1998;25:201–12.